Journal of Water Resource and Protection, 2024, 16, 640-670
https://www.scirp.org/journal/jwarp
ISSN Online: 1945-3108
ISSN Print: 1945-3094

Use of Groundwater, Baseflow and SPEI to Evaluate Water Resources in Michigan, USA

Sawyer Schnettler, Alexis Sonnemann, Katherine Clancy

College of Natural Resources, University of Wisconsin at Stevens Point, Stevens Point, USA
Email: kclancy@uwsp.edu

How to cite this paper: Schnettler, S., Sonnemann, A. and Clancy, K. (2024) Use of Groundwater, Baseflow and SPEI to Evaluate Water Resources in Michigan, USA. *Journal of Water Resource and Protection*, **16**, 640-670.
https://doi.org/10.4236/jwarp.2024.1610037

Received: September 7, 2024
Accepted: October 28, 2024
Published: October 31, 2024

Abstract

Precipitation and evaporation are commonly used to assess and forecast droughts. However, surface and groundwater respond to both land surface processes, land use, and climatic variables, and should be integrated into water management decisions. Water trend analysis near the Great Lakes is limited due to fluctuating cycles and data scarcity. In this study, we examine daily discharge data from 46 surface water gauges with high baseflow contributions and groundwater elevation from 28 observation wells in Michigan. Using established hydrograph separation techniques, we determined baseflow and standardized both annual average baseflow levels (SDBF) and groundwater levels (SDGW) from 1960 to 2022. These results are compared to the widely used Standardized Precipitation-Evapotranspiration Index (SPEI). SPEI is a widely used drought indicator that integrates both precipitation and potential evapotranspiration, offering a more comprehensive measure of water balance. While the SPEI suggests that Michigan is becoming wetter, the SDBF shows a mix of both wet and dry conditions. Interpreting SDGW is more challenging due to incomplete records, but it indicates varying groundwater stability across the state. In some areas, SDGW mirrors the trends seen in SDBF, while in others, it takes 3 to 4 years for groundwater levels to reflect the same changes observed in baseflow. Overall, SDBF provides a better understanding of surface processes and responses to changing climatic variables.

Keywords

SPEI, Drought, Groundwater, Baseflow

1. Introduction

The Great Lakes Region, surrounding Michigan, is experiencing significant climatic shifts due to global climate change, as evidenced by increasing temperatures,

changing precipitation patterns, and their impacts on water levels and ecosystems [1] [2]. The average temperature in the Great Lakes region has increased by about 1.5˚F over the past century, with projections indicating further warming [1] [2]. This warming has a profound impact on the hydrological cycle, leading to higher evaporation rates and altered precipitation patterns. As a result, extreme weather events, including severe rainfall and prolonged droughts, have become more common and intense [3]. Additionally, the Great Lakes region has seen a rise in winter precipitation but a decline in summer precipitation [4]. These changes are not only affecting water availability but are also influencing the region's hydrological balance, with implications for both surface and groundwater resources [5] [6].

The impacts of groundwater overuse in Michigan are significant, affecting water availability and quality. Research has shown that excessive groundwater extraction has led to declining aquifer levels, reduced streamflow, and deterioration in water quality [3]. Groundwater overdraft, particularly in high-demand areas, has resulted in decreased aquifer recharge rates and altered surface water interactions [5] [6]. Additionally, the combined effects of groundwater overuse and climate change have exacerbated water scarcity issues in Michigan. Increased evapotranspiration rates and variable precipitation patterns further strain groundwater resources, highlighting the need for sustainable management practices and effective monitoring [6].

Our understanding of the region's hydrology and its response to climatic changes is severely limited due to the scarcity of available data, as demonstrated by studies that point to the lack of comprehensive hydrological records in the Great Lakes region [1] [2]. Our goal is to compare standardized observed data from streams and groundwater to standardized precipitation combined with a modeled evapotranspiration to determine how the variables compare to one another over time and space in Michigan. With high baseflow contributions to many of the stream in Michigan, we expect baseflow to be able to be used as a proxy where groundwater data is scarce.

We decided to limit the scope of our investigation to annual data. The complexities of using seasonal precipitation data stem from the variability and unpredictability inherent in seasonal weather patterns. This variability makes it challenging to discern clear trends and make consistent predictions for water resource planning and management [7]. Consequently, decision-makers often rely on annual precipitation data as it provides a more stable and aggregated view of overall water availability [8] [9]. While seasonal data is valuable for understanding specific periods of water scarcity or abundance, annual data helps in making more reliable assessments and decisions regarding water resource management.

The Standardized Precipitation-Evapotranspiration Index (SPEI) is a critical tool for assessing drought conditions as it integrates both precipitation and evapotranspiration data. This index provides a more comprehensive view of drought by accounting for the effects of increased temperatures on evapotranspiration, which can exacerbate drought conditions even when precipitation levels are

adequate [10] [11].

Recent applications of the SPEI index in Michigan and the Midwest have highlighted significant trends in drought severity and frequency. Bhatt *et al.* (2023) [12] utilized the SPEI index to analyze drought and climate extremes in the Great Lakes region, noting substantial fluctuations in drought severity linked to both variable precipitation and elevated temperatures. Similarly, Hammed *et al*, 2023 [13] found that the SPEI index effectively captured recent increases in drought severity in Michigan, attributing these trends to reduced precipitation and increased temperatures. SPEI is a proven tool in drought analysis, but it is often complemented by other hydrological indicators, such as baseflow data, to provide a more comprehensive understanding of groundwater conditions and long-term water availability in regions like Michigan.

Groundwater management relies heavily on historical data, but many regions, including Michigan, face challenges due to limited groundwater data. The scarcity of comprehensive groundwater monitoring networks complicates efforts to assess groundwater levels, recharge rates, and overall water availability [14]. To address these data limitations, researchers have increasingly turned to alternative methods, such as using baseflow data as a proxy [15].

Baseflow, which represents the portion of streamflow sustained by groundwater discharge, provides insights into groundwater recharge and long-term water availability. Standardized baseflow indices, which normalize baseflow data to account for natural variability, are useful for evaluating groundwater dynamics in data-scarce regions [15]. Studies like those by Ayers *et al.* (2021) [16] highlight the use of baseflow indicators for groundwater management in data-scarce regions of the Upper Midwest, including Michigan and Wisconsin.

Studies have demonstrated the effectiveness of baseflow separation techniques in estimating groundwater recharge and levels. For example, Clancy *et al.*, 2023 [17] explored baseflow data as a companion to stream flow and precipitation drought patterns in Wisconsin, providing insights into groundwater recharge in regions with limited data. Additionally, Manzano and Barkdoll (2022) [18] examined the use of baseflow data to estimate groundwater levels and recharge in the Great Lakes region, discussing methodologies and applications. These approaches offer valuable alternatives for groundwater assessment in the absence of extensive monitoring networks.

The research described in this paper builds upon the work of Manzano and Barkdoll (2022) [18] and Clancy (2023) [17]. The inclusion of annual standardized baseflow is expected to enhance our understanding of long-term groundwater dynamics and recharge patterns by providing a normalized measure of groundwater's contribution to streamflow. This approach is particularly valuable in regions where baseflow is a significant indicator of groundwater levels, as it offers a more comprehensive view of how precipitation and evapotranspiration trends impact groundwater resources over time. By integrating baseflow data with annual groundwater measurements and SPEI, which captures the balance between

precipitation and evapotranspiration, we aim to clarify the complex interactions between meteorological variables and water availability. Our research addresses the challenges posed by limited groundwater data and allows for a more nuanced analysis of annual hydrological and drought patterns across the Great Lakes region.

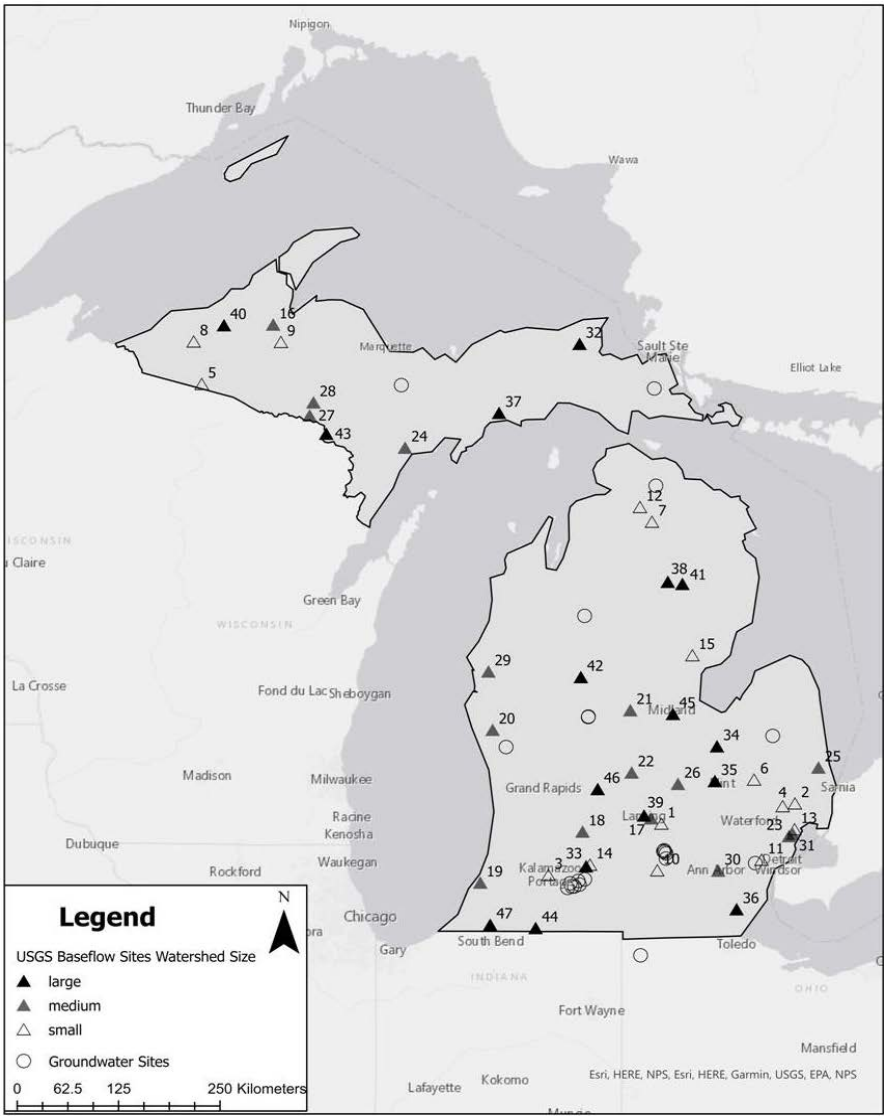

Figure 1. Location of USGS surface water (baseflow) sites and groundwater wells in the state of Michigan.

2. Study Area

Lower Michigan is surrounded by the Great Lakes on all three sides, and Upper Michigan is surrounded on north and south by Great Lakes as shown in Figure 1. Research that integrates precipitation, streamflow, and groundwater in the Great Lakes region is notably scarce [5] [6]. This is in part due to the complex nature of lake and shallow groundwater interactions, lack of appropriate temporal and

spatial resolution of gaging site data for groundwater and surface water, and lack of stationarity within long term data sets. We had four criteria for study selection criterion: First, stations required a length of continuous discharge record that was greater than 10 years. Second, stations were selected with a high baseflow component (>60 percent). Our third criterion was to find a range of watershed sizes. Our final criterion was to find sites that range from the northern, central, and southern parts of the state. Our selection resulted in 41 sites US Geological Survey Sites (USGS) [19] with a time continuous time span of 1960 to 2024 with an average baseflow component of 77 percent.

To account for the impact of size, we grouped them as follows: (small watersheds: 4.8×107 to 8.3×108 m^2; medium: 8.9×108 to 1.91×109 m^2; large: 2.0×109 to 9.5×109 m^2). Site location of the watersheds can be seen in **Figure 1**, and these data are summarized in **Table 1** and **Table 2**.

Finding appropriate groundwater sites proved significantly more challenging. We focused our search on unconfined aquifers with average water elevation levels within 30 feet of the land surface and only selected sites with ten or more years of continuous data. Applying these criteria, we narrowed down the 2,086 USGS observational well sites in Michigan to just 22 sites [19]. Most of these wells have records extending back to 2002 (22 years), except for one well that has continuous data starting from 1990.

To categorize our groundwater observation well and surface water gauging data locations, we used similar latitudes as Clancy, 2023 [17], where Northern locations are: above 44.5˚, Central locations: between 44.3˚ and 43.5˚, and Southern locations: below 43˚). We added a fourth category of "northern-up" which refers to the sites on the Upper Peninsula of Michigan (see **Figure 1** and **Table 1** and **Table 2**).

Table 1. USGS surface water stations for the state of Michigan, where Dev, For, Ag, and Wet, refer to landcover percentages of Developed, Forest, Agricultural, and Wetlands, respectively. Q (cms) refers to the average annual discharge in cubic meters per second. Location is determined by latitude, WS size refers to watershed size. Sign change refers to the number of isolated sign changes with the standardized record, as described in the text. All data have complete records from 1960-2023.

MAP ID	STATID	BFI	LAT	LONG	Location	Size (sq. m)	Relative Size	Sign Change
1	04112000	0.42	42.68	−84.36	south	2.42E+07	small	5
2	04164300	0.28	42.85	−82.88	south	3.37E+07	small	9
3	04106400	0.86	42.24	−85.61	south	4.84E+07	small	4
4	04164100	0.73	42.82	−83.02	south	5.65E+07	small	9
5	04037500	0.65	46.25	−89.45	northern	1.31E+08	small	9
6	04146000	0.71	43.04	−83.34	central	1.43E+08	small	9
7	04128990	0.83	45.16	−84.47	northern	1.49E+08	small	12
8	04036000	0.78	46.59	−89.54	northern	4.20E+08	small	7
9	04040500	0.69	46.58	−88.58	northern	4.43E+08	small	11
10	04109000	0.79	42.28	−84.41	south	4.51E+08	small	3
11	04166500	0.48	42.37	−83.25	south	4.84E+08	small	12

Continued

12	04127997	0.89	45.27	−84.60	northern	4.97E+08	small	10
13	04164500	0.47	42.63	−82.89	south	5.15E+08	small	16
14	04105000	0.76	42.33	−85.15	south	6.24E+08	small	9
15	04142000	0.76	44.07	−84.02	central	8.29E+08	small	7
16	04041500	0.66	46.73	−88.66	northern	8.96E+08	medium	10
17	04112500	0.67	42.73	−84.48	south	9.19E+08	medium	10
18	04117500	0.73	42.62	−85.24	south	9.97E+08	medium	10
19	04102500	0.87	42.19	−86.37	south	1.01E+09	medium	5
20	04122200	0.86	43.46	−86.23	central	1.05E+09	medium	13
21	04154000	0.81	43.63	−84.71	central	1.08E+09	medium	13
22	04115000	0.72	43.11	−84.69	central	1.12E+09	medium	8
23	04164000	0.67	42.58	−82.95	south	1.15E+09	medium	19
24	04059500	0.73	45.75	−87.20	northern	1.17E+09	medium	7
25	04159492	0.43	43.15	−82.62	central	1.20E+09	medium	11
26	04144500	0.73	43.02	−84.18	central	1.39E+09	medium	17
27	04062000	0.76	46.01	−88.26	northern	1.63E+09	medium	3
28	04062500	0.79	46.11	−88.22	northern	1.70E+09	medium	3
29	04122500	0.89	43.95	−86.28	central	1.76E+09	medium	14
30	04174500	0.80	42.29	−83.73	south	1.89E+09	medium	10
31	04165500	0.62	42.60	−82.91	south	1.90E+09	medium	12
32	04045500	0.85	46.57	−85.27	northern	2.05E+09	large	14
33	04105500	0.82	42.32	−85.20	south	2.13E+09	large	12
34	04151500	0.57	43.33	−83.75	central	2.18E+09	large	13
35	04148500	0.69	43.04	−83.77	central	2.48E+09	large	10
36	04176500	0.64	41.96	−83.53	south	2.70E+09	large	5
37	04056500	0.87	46.03	−86.16	northern	2.85E+09	large	11
38	04136000	0.91	44.68	−84.29	northern	2.87E+09	large	3
39	04113000	0.75	42.75	−84.56	south	3.19E+09	large	11
40	04040000	0.69	46.72	−89.21	northern	3.47E+09	large	5
41	04136500	0.89	44.66	−84.13	northern	3.52E+09	large	9
42	04121500	0.86	43.90	−85.26	central	3.71E+09	large	2
43	04063522	0.80	45.87	−88.07	northern	4.66E+09	large	10
44	04099000	0.85	41.80	−85.76	south	4.83E+09	large	8
45	04156000	0.61	43.60	−84.24	central	6.22E+09	large	12
46	04116000	0.77	42.97	−85.07	south	7.36E+09	large	16
47	04101500	0.87	41.83	−86.26	south	9.49E+09	large	7

Table 2. USGS observation wells for groundwater. Ave(m) refers to the average groundwater depth below the surface, and Std (m) refers to the standard deviation of the groundwater depth. Location was determined by latitude.

Groundwater ID	Ave (m)	Std (m)	Location	Year	Lat	Long
415602084593701	4.86	1.48	southern	2002	41.56	−84.59
423114090161101	21.65	0.83	southern	2002	42.13	−85.40
423717089120901	1.55	0.16	southern	2002	42.13	−85.40
435142089270101	9.78	0.76	southern	2002	42.13	−85.40
425006088271501	7.35	0.59	southern	2002	42.14	−85.35
425246091042101	2.81	1.30	southern	2003	42.14	−85.35
435244089293401	5.49	0.88	southern	2002	42.14	−85.35
425246091042102	17.37	1.16	southern	2002	42.14	−85.38
425246091042103	4.22	1.06	southern	2003	42.15	−85.33
425246091042104	1.36	0.65	southern	2003	42.16	−85.27
425551090391301	9.63	0.44	southern	2003	42.16	−85.35
425607088173001	5.00	0.65	southern	2002	42.16	−85.35
425613088014301	0.90	0.31	southern	2002	42.17	−85.37
430409089234601	4.33	0.42	southern	2002	42.19	−85.28
430416088144301	8.16	0.23	southern	2002	42.21	−85.21
430456089190602	6.85	0.44	southern	2002	42.34	−83.32
430718089291501	3.00	0.45	southern	2002	42.38	−84.31
431233089103201	6.05	0.37	southern	2002	42.42	−84.31
430416088144603	4.99	0.94	southern	2002	42.44	−84.33
431312089475301	3.14	0.61	southern	2018	42.44	−84.34
432415088552601	3.44	0.24	southern	2022	42.45	−84.33
433921091132101	2.19	0.84	central	2018	43.31	−86.08
433921091132102	5.00	0.89	central	2018	43.41	−83.13
433921091132103	3.22	0.40	central	2002	43.56	−85.17
433956089275601	10.43	1.07	central	2002	43.57	−85.17
434342090495601	11.33	0.39	central	2002	44.39	−85.21
434551089365001	2.17	0.91	northern	2018	45.44	−84.42
434944089345001	3.03	0.89	northern	2002	46.22	−84.44

3. Methods

3.1. SPEI

SPEI data, available in the public domain, are provided in a spatial-time format called NetCDF, which consists of gridded spatial (raster) layers, each representing a specific time slice, typically at a monthly resolution (SPEI citation) [11]. For Michigan, SPEI data are available from 1901 - 2022 with a 0.5-degree resolution. SPEI-12 was the best time scale to correlate with baseflow. SPEI values for the

study watersheds were obtained for a 12-month timescale. Data methodology are found in [10] [20]. Data extraction methods and analysis of SPEI time scales are described in detail in [20].

3.2. Baseflow and Groundwater Data

In April 2023, we accessed the USGS national water database to obtain both daily flow data and groundwater elevation measurements [18]. As mentioned in the site selection, shallow groundwater sites with connection to surface water and watersheds with high baseflow were selected. Stream stations with complete years of record for streamflow from 1960 - 2022 were selected. Groundwater stations were selected with 10 years of continuous data with data dating back to 2002.

In the current study, we utilized the same baseflow separation method detailed in Clancy's (2023) [17] research. This method involves the use of the USGS's Hydrograph Separation and Analysis (HYSEP) [20] program for streamflow separation, which, despite newer advancements like stable isotope analysis and temperature sensor methods, remains a practical and widely used tool. Clancy's (2023) [17] research provides a broader discussion of baseflow separation methods [21].

Annual averages of groundwater and baseflow data were derived from years with complete daily data. Annual groundwater and baseflow data were standardized using the standard departure to calculate the standard departure of annual groundwater values (SDGW) and the standard departure for baseflow (SDBF). The formula for calculating SDGW and SDBF is shown in Equation (1).

$$SD = \left(x_i - \mu\right)/\delta \tag{1}$$

In Equation (1), SD is the standard departure for the dataset (either SDGW or SDBF) and xi represents the log of the annual value for one year, μ represents the average of the log of the annual dataset, and σ is the standard deviation of the log of the annual dataset.

3.3. Watershed Delineation and LandCover

The delineation of the 46 watersheds in the study area was conducted using the D8 method, a widely recognized approach available in ESRI's ArcGIS Pro (version 3.3) Hydrology Tools. This method, as described by Troolin and Clancy (2016) [22] and originally developed by Jenson (1984) [23], requires only elevation data, such as digital elevation models (DEMs), and an outlet point for successful delineation of the study watersheds. For this study, we utilized a 30-meter digital elevation model provided by the USGS [24]. The resulting watershed areas and perimeters were compared with USGS-published values, and they matched within 99%, confirming the accuracy of the delineation. Additionally, land cover data was obtained from the USGS at a 30-meter resolution, which allowed us to calculate the percentages of urban, agricultural, wetland, and forested areas within each watershed [25].

3.4. Raster Generation

To generate the necessary rasters, we combined the locations of USGS stream

gauging stations and groundwater observation wells with Hydrologic Unit Codes (HUCs), specifically HUC-12s. The HUC system, managed by the U.S. Geological Survey (USGS) and the U.S. Environmental Protection Agency (EPA), is a standardized classification system used in the United States to identify and manage watersheds and river basins. This system enables effective monitoring and analysis of water resources across various scales, from large river basins to smaller, localized watersheds. The hierarchical structure of HUCs, ranging from Regions (2-digit HUC) to more granular levels like HUC-12, allows for a comprehensive understanding of the nation's hydrologic systems [26].

After spatially joining the relevant data, we used the polygon-to-raster tool in ArcGIS Pro 3.3 to create rasters for each year, corresponding to SDBF, SDGW, and SPEI. We outline the method in **Figure 2**. Given the large volume of data. To simplify the values of SPEI, SDBF and SDGW we converted all the data into positive or negative values to examine broad trends and more easily discern where there are spatial differences where there are complete data for all three variables for 10 years.

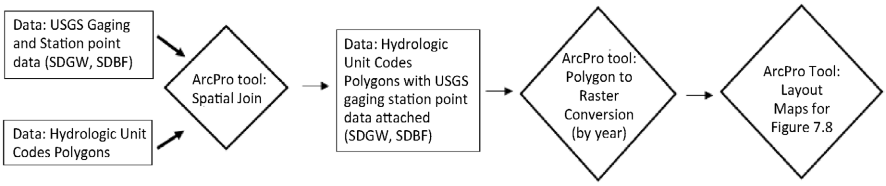

Figure 2. Method flow chart.

3.5. Standardization of Baseflow and Groundwater Data

Baseflow data were log-transformed for standardization, allowing for better comparison across different watersheds and improved trend visibility. The standard departure for baseflow (SDBF) was developed using the log-transformed annual mean, with the standard deviation and mean calculated for the annual dataset. The choice of data distribution is informed by Vicente-Serrano *et al.* (2012) [10] [27]. Similarly, groundwater elevations were standardized for the 2002 to 2022 period to allow values to be comparable across time and space. Details on the data distribution and standardization are described in detail in Clancy 2023 [17].

3.6. Isolate Sign Change

In this analysis, we utilized a standardized index that ranges continuously, with increasingly negative values indicating drier conditions and increasingly positive values reflecting wetter conditions. While the index values exist on a continuum, we specifically focused on evaluating isolated sign changes within the annual data for SDBF, SDGW, and SPEI. An isolated sign change was defined as a single negative or positive value flanked by values of the opposite sign. Isolated sign changes refer to a value in the data set that have a different value than those surrounding

it. For example, the series 1, 1, −1, −1 have no isolated sign changes, but the series 1, 1, −1, 1 has one isolated sign change. This approach, previously utilized in studies to assess drought variability and detect underlying climatic trends [10] [28] was employed to evaluate the system's variability, potentially revealing a flashiness that may obscure underlying trends.

The concept of isolated sign changes in climate or drought data analysis is not commonly employed as a standalone method but is sometimes applied in broader analyses of climate variability or extreme events. For instance, Vicente-Serrano *et al.* (2010) [10] explored the importance of capturing short-term fluctuations and extremes within the Standardized Precipitation Evapotranspiration Index (SPEI), which aligns with the idea of using isolated sign changes to detect variability in drought conditions. Similarly, Wang *et al.* (2020) [28] investigated temporal and spatial drought trends in northern Shaanxi, China, using indices like SPEI, indirectly addressing variability through methods that could encompass isolated sign changes.

3.7. Mann-Kendall Trend Test

The overall trends in SDBF, SDSF, and SPEI time series data were evaluated using the Mann-Kendall tau trend test [29], implemented through the Kendall R package [30]. The Mann-Kendall test is a non-parametric statistical hypothesis test that uses the rank of the data to detect trends, making it particularly useful for hydrological time series analysis [31] [32]. This test has gained widespread acceptance in hydrology due to its inclusion in statistical manuals for hydrologists and its flexibility in examining the stationarity of various climate variables [33].

For the Mann-Kendall hypothesis test, the null hypothesis (H_0) assumes the data are random (indicating no trend), while the alternative hypothesis suggests a trend (either upward or downward). An alpha level of 0.05 was used, with p-values less than 0.05 indicating the presence of a trend. The direction of the trend was generally determined by graphical analysis. A limitation of the Mann-Kendall tau trend test is its assumption of a monotonic trend, meaning it can only detect a single trend direction. Data with multiple trends may often result in a "no trend" conclusion. For datasets exhibiting complex trends, involving both upward and downward movements, it is recommended to divide the data into subsets and analyze them separately. The main purpose of applying the Mann-Kendall test in this study was to examine and compare the trend results (e.g., "no trend" or "trend") across the watershed datasets (SDBF, SPEI, SDSF) [17].

3.8. Correlation

The SDBF were evaluated using several metrics. Linear correlation was used to test the relationship between SDBF, SDGW, and SPEI. Additionally linear correlation was used to examine isolated sign changes in SDBF and landuse percentages, BFI, watershed size, and watershed location. To obtain Pearson correlation coefficients (R2) values, we used the cor function in R 4.4.1.

3.9. Run Theory

A common method for characterizing drought persistence is time-series run theory [34], which calculates the number of consecutive occurrences of a specific value (either negative or positive). In this study, data were classified as either positive or negative. Custom R scripts were used to determine the maximum run lengths for negative and positive values in SDBF, SDSF, and SPEI data across all watersheds. Additionally, the year corresponding to the maximum run length was recorded for each watershed. This analysis helps to assess the consistency of data within each watershed and identify patterns across different watersheds [10] [17] [34]. Seflow data were log-transformed for standardization, allowing for better comparison across different watersheds and different hydrologic data.

4. Results

4.1. Land Cover Summary

The study includes a diverse range of sites, characterized by varying watershed sizes and land use distributions as summarized in Table 1. On average, the development (Dev) across these sites is 18.5%, indicating a moderate level of urban influence. Forest cover (For) averages 27.6%, reflecting significant but variable forest presence within the watersheds. Agricultural land (Ag) constitutes 27.4% on average, showing a substantial portion of land used for farming. Wetlands (Wet) cover an average of 22.7% of the watersheds. The average discharge rate (Q) across all sites is 39.8 cubic meters per second.

In the Northern region, the average development is relatively low at 16.5%, with the highest proportion of forest cover at 31.1% and significant agricultural land use at 29.0%. Wetlands also constitute 22.9% of the land. The Central region shows a moderate level of development at 22.7%, combined with a balanced mix of land uses: 24.7% forest, 27.6% agriculture, and 20.6% wetlands. In contrast, the Southern region experiences higher development (22.0%) and a slightly higher proportion of wetlands (24.3%), with forest and agriculture coverage at 26.2% and 27.3%, respectively.

4.2. Baseflow Summary

The Baseflow Index (BFI) varies across Michigan's regions, reflecting differences in groundwater contribution to streamflow (Table 1). In the Northern region, the average BFI is 0.73, indicating a relatively high proportion of streamflow derived from groundwater. The BFI values in this region range from 0.42 to 0.89, suggesting variability in groundwater contributions across different sites. The Central region has a slightly lower average BFI of 0.64, with values ranging from 0.42 to 0.89. The Southern region shows an average BFI of 0.67, with values spanning from 0.28 to 0.89.

4.3. Isolated Sign Change

SDBF had the highest incidence of isolated sign changes with 9.5 as the average, and a minimum of 3 and a maximum of 19 during the 1960 - 2022 period (summarized in Table 1). Comparatively, SPEI had an average of 6.9 isolated sign changes with a

minimum of 4 and a maximum of 11. SDGW isolated sign changes can only be examined during the 2013 - 2022 period, so are not comparable for the entire record.

To determine local surface impacts on SDBF, we examined the watershed's landcover percent for wetland, forest, urban, and agriculture. We also examined watershed location by latitude, and watershed size. All landcover correlations between isolated sign change and landcover were not significant. The highest value was only 0.22 (for wetlands). The isolated sign changes for location and watershed size also proved insignificant.

When we examine ten years of data (2013 - 2022) for SDBF and SPEI, SPEI's isolated sign change value of 2.1 is the highest compared to SDBF's value of 1.7. SDGW's value of isolated sign changes is the lowest at 1.1.

4.4. Mann Kendall Summary

The Mann-Kendall tau trend test results across Michigan's regions reveal diverse patterns in precipitation trends. In the southern region, most sites exhibit significant increasing trends over the long term. Sites such as 04099000 and 04166500 demonstrate consistent increasing trends, whereas sites like 04102500 and 04105500 show no significant trends in the recent decade, despite long-term increases. In contrast, the central region also shows several sites with significant increasing trends. The northern region presents a more varied picture: while sites like 4062000 show significant increases, many others, including 04059500 and 04063522, display no significant trends.

As shown in Figure 3, the total data analysis, which spans data from 1960 to 2022, highlights a general pattern of increasing precipitation in the southern and central regions. The shorter period 2013 to 2022, uncovers different trends. For instance, site 04102500 shows an increasing trend over the long term but no significant recent trend. Similarly, while the southern and central regions exhibit a consistent pattern of increase, the northern region shows a mix of increasing trends and no significant trends. These variations highlight the differences in trend patterns over different time periods and across regions, reflecting both enduring long-term increases.

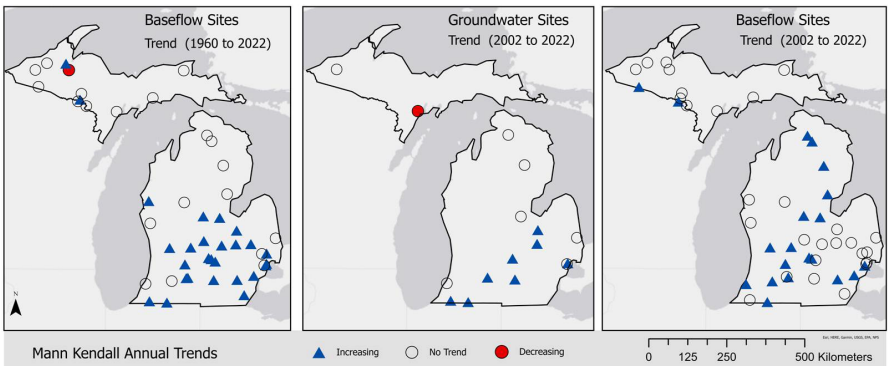

Figure 3. Results of Mann Kendall Annual trend test for Baseflow Sites (SDBF) for 1960 to 2022, groundwater Sites (SDGW) for 2002 to 2022 and baseflow Sites (SDBF) for 2002 to 2022. Legend indicates the direction of trend.

4.5. Mann Kendall Summary: Groundwater Trends Compared to Precipitation

In the southern region, there is a notable alignment between groundwater and baseflow trends. For instance, site 04099000 shows increasing trends in both groundwater (p-value of 0.0311) and baseflow. Similarly, site 04101500 displays an increasing trend in groundwater (p-value of 0.0053), which corresponds with a long-term increasing trend in baseflow (p-value of 0.0011), although recent baseflow data shows no significant trend. At site 04105500, groundwater trends are increasing (p-value of 0.0056), aligning with the long-term baseflow increase (p-value of 0.0001), though recent baseflow data show no significant change. Site 4109000 exhibits a consistent increasing trend in both groundwater (p-value of 0.0018) and baseflow (p-values of 0.0012), reflecting a strong, synchronized trend across both metrics.

In contrast, the northern region presents a more varied picture. For example, site 04036000 shows no significant trend in groundwater (p-value of 0.3837) and also no significant baseflow trend (p-value of 0.6780), indicating stability in both metrics. Site 04059500 shows a decreasing groundwater trend (p-value of 0.0228), while long-term baseflow trends remain stable (p-value of 0.0833), highlighting a divergence in groundwater and baseflow trends. At site 04127997, groundwater shows no significant trend (p-value of 0.1929), whereas long-term baseflow trends are increasing (p-value of 0.6867), demonstrating a discrepancy between groundwater and baseflow patterns.

The central region also reveals mixed trends. For instance, site 04148500 has an increasing groundwater trend (p-value of 0.0195), which aligns with an increasing long-term baseflow trend (p-value of 0.0282). However, recent baseflow trends indicate no significant change. Similarly, site 04151500 shows increasing trends in both groundwater (p-value of 0.0325) and long-term baseflow (p-value of 0.0119), with recent baseflow trends showing no significant change. At site 04156000, the groundwater trend is less significant (p-value of 0.1050), whereas the long-term baseflow trend is increasing (p-value of 0.0003).

Overall, the comparison reveals that the southern region shows a strong agreement between increasing trends in groundwater and baseflow, though recent baseflow data sometimes diverge. In the northern region, discrepancies between decreasing groundwater and stable baseflow trends are apparent. In the central region, while long-term trends in groundwater and baseflow often align, recent trends display variability.

4.6. Mann Kendall Trend Test Results Map

As shown in **Figure 3**, the Mann Kendall Trend overall agreement between SDBF and SDGW. SDBF for the years 1960 to 2022 (**Figure 3**, far left figure) has increasing trends in the central and southern portion of the state, but no trend results in the north and much of the Upper Peninsula, with one decreasing trend. Examining only the 2002 to 2022 period for SDBF indicates that there are more increasing trends in the northern part of the state. Overall, the Upper Peninsula results are similar to the

entire record from 1960 to 2022. SDGW matches a little better the longer-term record of SDBF with both variables indicating no trends in the Northern part of the state.

4.7. Correlation

SDBF and SDGW for the 1960 to 2022 period correlated with an average of 0.70. The minimum was a 0.43 and the max was 0.83. Using a lag of 1 year, where SPEI values for 1960 were correlated with SDBF values of the following year, resulted in a correlation of 3 percent lower than the matched year correlation.

Correlation between SDBF and SDGW from the 2013 to 2022 period was highly variable with values as high as 0.94 and as low as 0.47, with an average of 0.52. The correlation between SDGW and SPEI were considerably lower with values as high 0.62 and as low as 0.12, with an average of 0.28. SDBF and SPEI correlation were low with an average value of 0.28, with maximum of 0.35 and a minimum of -0.13.

4.8. Runs Summary: SDBF

In the Northern region, positive run lengths for sites varied from 5 to 21 years, with many sites beginning their longest positive runs in the 1960s and early 2000s (Table 3). Negative runs were also notable, ranging from 4 to 16 years, often starting in the early 2000s or late 1990s. For example, Station 04062000 experienced an extended positive run of 21 years starting in 2002, juxtaposed with a significant 16-year negative run starting in 1980. Similarly, Station 04045500 had a lengthy 11-year positive run beginning in 1965 and a shorter 4-year negative run starting in 1961. A representative station is shown in Figure 4 for comparison to regional SDGW and SPEI.

In the Southern region, stations showed a mix of positive run lengths from 5 to 10 years, with many initiating their longest positive runs in the late 1980s to early 2010s (Table 3). A representative station is shown in Figure 5 for comparison to regional SDGW and SPEI values. Negative runs varied from 7 to 15 years, often starting in the 1960s or 1990s. For instance, Station 04105000 had a prominent 10-year positive run starting in 2013, contrasting with a 9-year negative run beginning in 1960. Station 04116000 displayed a 5-year positive run starting in 1972 and a substantial 12-year negative run starting in 1960.

Table 3. Summarizes the max negative and positive runs as well as the year the run started for SPEI and SDBF by region. Due to lack of data outside of the southern regions, all GW data were compiled.

Region, variable	Max Negative Run Length	Max Negative Start Year	Max Positive Run Length	Max Positive Start Year
southern, SPEI	5	1966	9	2002
southern, SDBF	9	1963	6	1988
central, SPEI	4	1969	9	1999
central, SDBF	8	1968	6	1991
northern, SPEI	6	1993	9	1995
northern SDBF	11	1993	9	1979
all regions, SDGW	6	1982	6	1986

In the Central region, positive runs ranged from 5 to 8 years, with many beginning in the 1980s to early 2010s (Table 3). A representative station is shown in Figure 6 for comparison to regional SDGW and SPEI values. Negative runs varied between 6 and 13 years, frequently starting in the 1960s or 1990s. Notably, Station 04144500 had a 7-year positive run starting in 2016 and a 13-year negative run beginning in 1960, while Station 04156000 had an 8-year positive run starting in 2013 with a 7-year negative run beginning in 1960.

4.9. Runs Summary: SDGW

Across all locations, the average start date for negative runs is generally in the late 1970s to early 1980s. The average length of negative runs varies by location, with the South showing the longest average length at approximately 6 to 7 years, followed by the Central region with an average of about 4 years. The North has a slightly shorter average length of around 5 to 6 years. This indicates that negative trends, characterized by declines in groundwater levels, tend to start during a similar period across locations but differ in duration, with the South experiencing the most prolonged negative periods.

For positive runs, the average start date spans from the late 1970s to early 1980s. However, the average length of positive runs is more variable. The South generally experiences longer positive runs, averaging around 7 to 8 years, while the Central region averages about 5 to 6 years. The North has shorter positive runs, averaging around 4 to 5 years. This suggests that positive trends, which reflect increases in groundwater levels, also begin in a similar timeframe across locations but differ in duration, with the South showing the most extended positive trends.

Overall, while the start dates for both positive and negative runs are clustered around the late 1970s to early 1980s, the lengths of these runs vary, with the South exhibiting the longest periods of both negative and positive trends compared to the Central and North regions (Table 3).

4.10. Runs Summary: SPEI

In the North region, the average maximum negative run length is approximately 6.2 years, with the longest negative runs starting around 2003. The average maximum positive run length is about 6.7 years, with notable runs beginning in 2013. This region displays a diverse range of negative and positive run lengths, with some periods of extended drought and wet conditions. The variability reflects a range of climatic conditions over several decades.

For the Central region, the average maximum negative run length is around 3.8 years, with negative runs generally starting between 1961 and 1980. The average maximum positive run length is about 5.5 years, with positive runs typically beginning from 1976 to 2013. The Central region tends to experience shorter negative runs and somewhat variable positive runs. The shorter durations of negative runs and a broader range of positive runs highlight a relatively stable yet variable climate pattern.

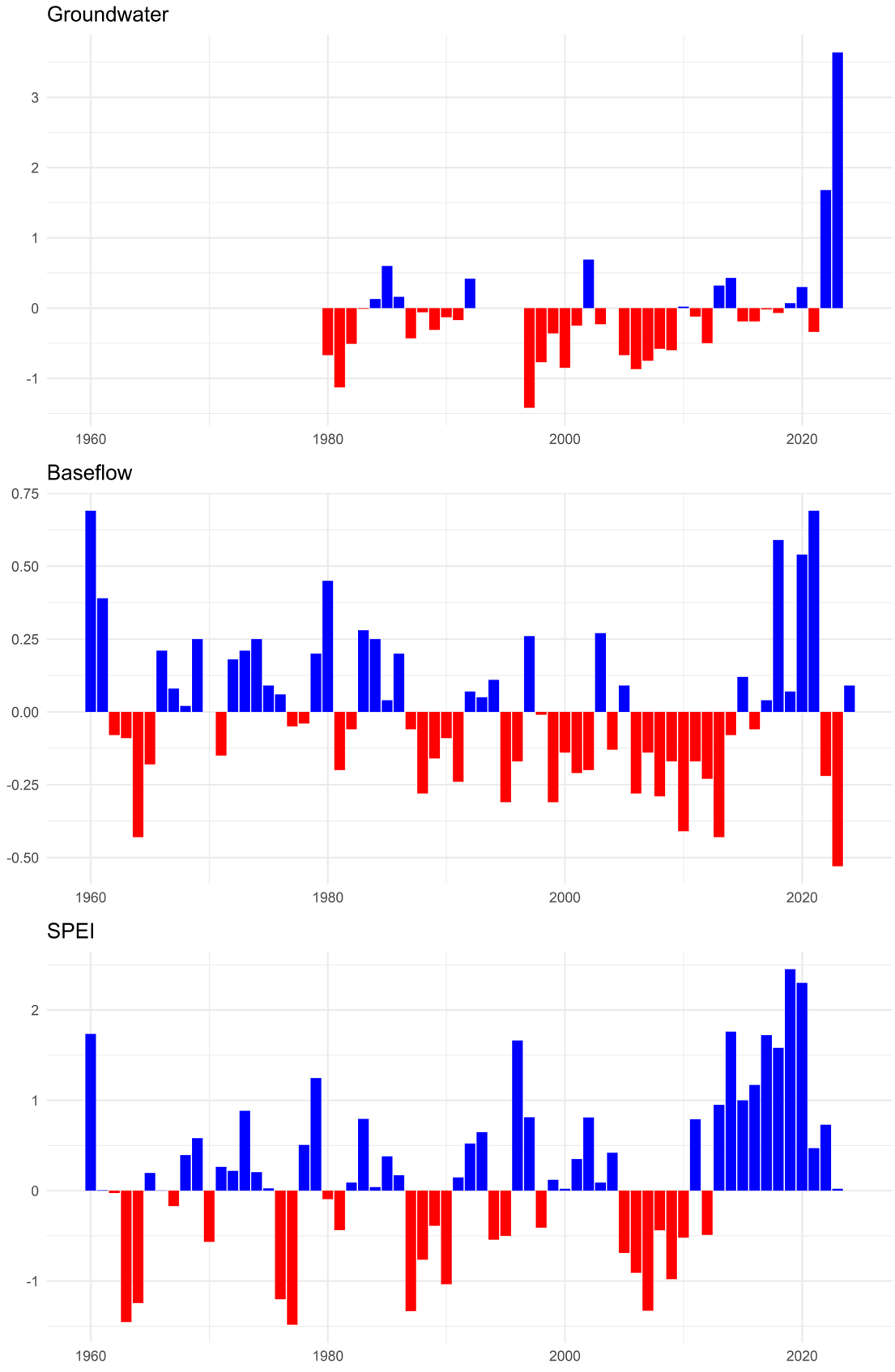

Figure 4. SPEI, Baseflow and Groundwater Flow for north.

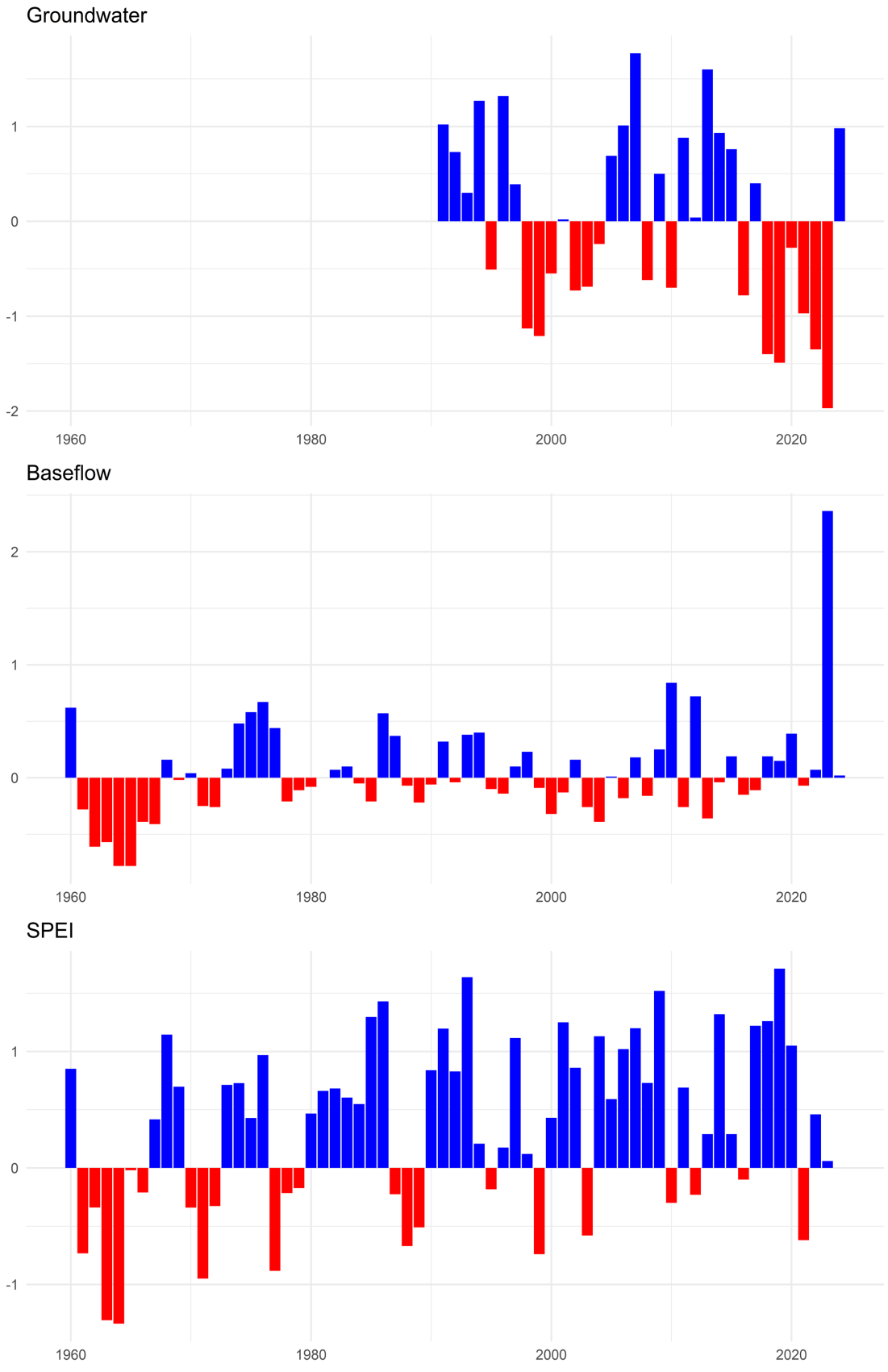

Figure 5. SPEI, Baseflow and Groundwater Flow for south.

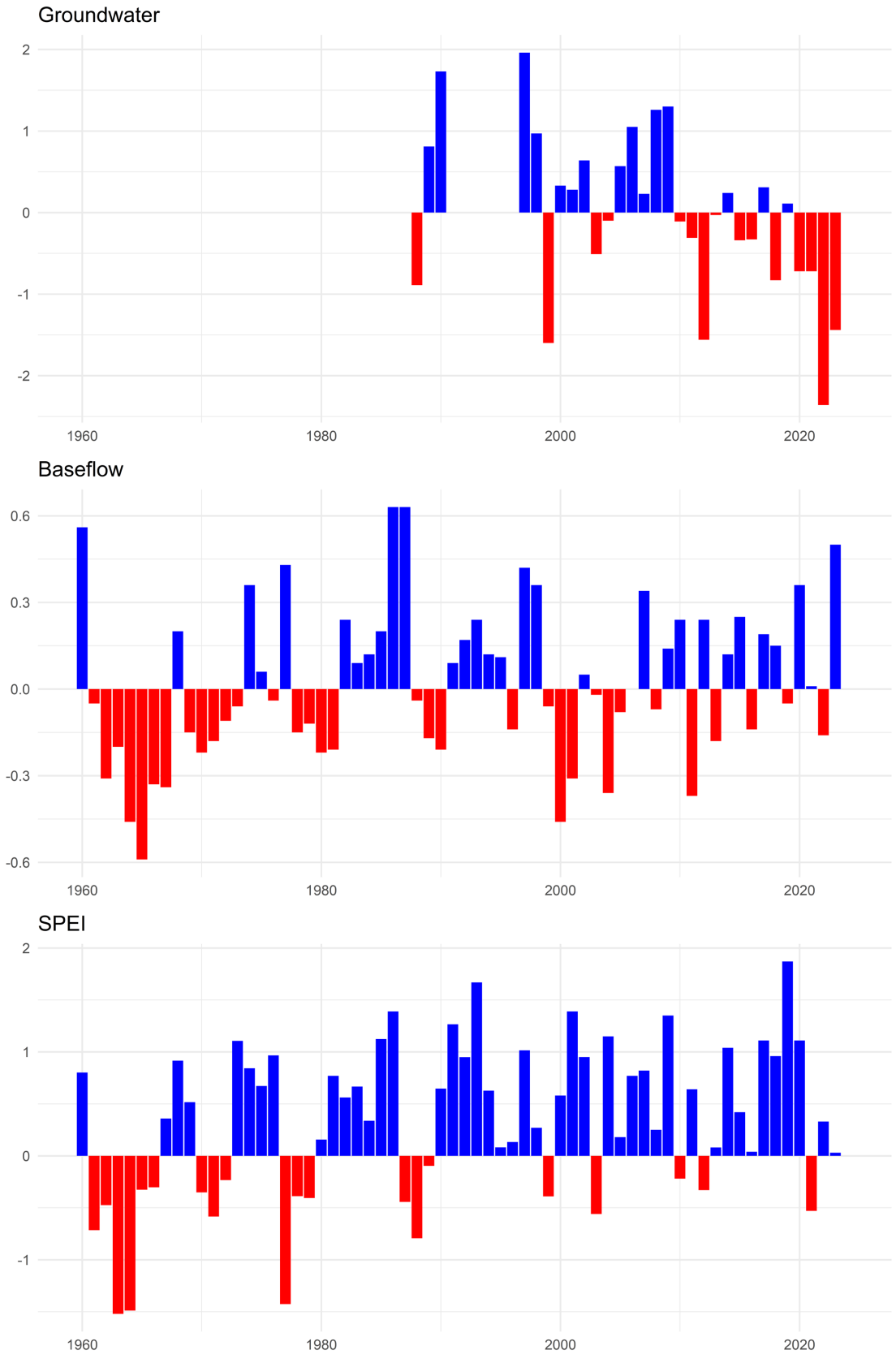

Figure 6. SPEI, Baseflow and Groundwater Flow for central.

In the Southern region, the average maximum negative run length is approximately 6.2 years, with many of the longest negative runs starting in 1961. The average maximum positive run length is about 8.0 years, with significant runs beginning between 1961 and 2013. The Southern region shows the longest periods of both negative and positive runs, indicating extended periods of drought and wet conditions over the decades. This reflects a notable variability in hydrological conditions, with the longest runs starting predominantly in the 1960s and extending into the 2000s.

In summary, while the North experiences a diverse range of both short and long runs, the Central region has shorter negative runs and somewhat variable positive runs. The Southern region exhibits notably long periods of both negative and positive runs, suggesting a more pronounced variability in hydrological conditions over time (Table 3).

4.11. Statistical Comparison of SPEI, SDBF, SDGW

In the North region, SPEI values, groundwater trends, and baseflow run lengths exhibit a consistent pattern where positive runs often correspond with increasing groundwater levels and longer baseflow periods. The average negative run length for SPEI is about 6.2 years, with significant negative runs typically starting around 2003, while positive runs average 6.7 years and begin around 2013. Groundwater trends in this region generally show either no significant trend or slight decreases during negative runs, aligning with shorter negative baseflow periods averaging 5 to 7 years. Conversely, positive groundwater trends often match with longer positive baseflow periods, reflecting periods of increased water availability.

In the Central region, the SPEI values show shorter negative run lengths, averaging 3.8 years, with negative runs beginning between 1961 and 1980. Positive run lengths average 5.5 years, with these runs generally starting from 1976 to 2013. This region's groundwater trends typically display little to no change or slight decreases during negative periods, and positive trends align with longer positive SPEI runs. Baseflow data in Central shows shorter negative run lengths, about 3 to 6 years, and longer positive run lengths averaging 6 to 10 years, indicating a relatively stable climate with a clear pattern of extended positive conditions.

The Southern region is characterized by significant variability, with both negative and positive run lengths extending over long periods. SPEI values indicate an average negative run length of 6.2 years and positive run length of 8.0 years, with notable runs beginning between 1961 and 2013. Groundwater trends in this region show more variability, with extensive negative trends and strong increases during positive periods. Baseflow run lengths are similarly long, averaging 6 to 10 years for both negative and positive runs, reflecting the region's pronounced climate variability.

4.12. Spatial Comparison of SPEI, SDBF, SDGW

To simplify the values of SPEI, SDBF and SDGW we converted all the data into positive or negative values to examine broad trends and more easily discern where there are spatial differences where there are complete data for all three variables

for 10 years.

As shown in Figure 7 and Figure 8, the comparison of SDBF (Standardized Baseflow) and SDGW (Standardized Groundwater) responses is of particular interest. Annual SPEI values are predominantly positive, with exceptions in 2016 (a slightly drier year) and 2021 (a drier year). Notably, SDBF and SDGW exhibit more nuanced patterns compared to the annual SPEI values. In 2021, 2018, 2017, and 2016, SDGW reflects drier conditions in the northern part of Michigan, diverging from the spatial patterns observed in SDBF. SDGW shows a degree of inertia, with dryness in the northern region persisting from 2018 to 2016. Although SDBF and SPEI indicated wetter conditions across much of the state in 2019 and 2020, SDGW remained drier in the southwestern portion of Michigan and the Upper Peninsula.

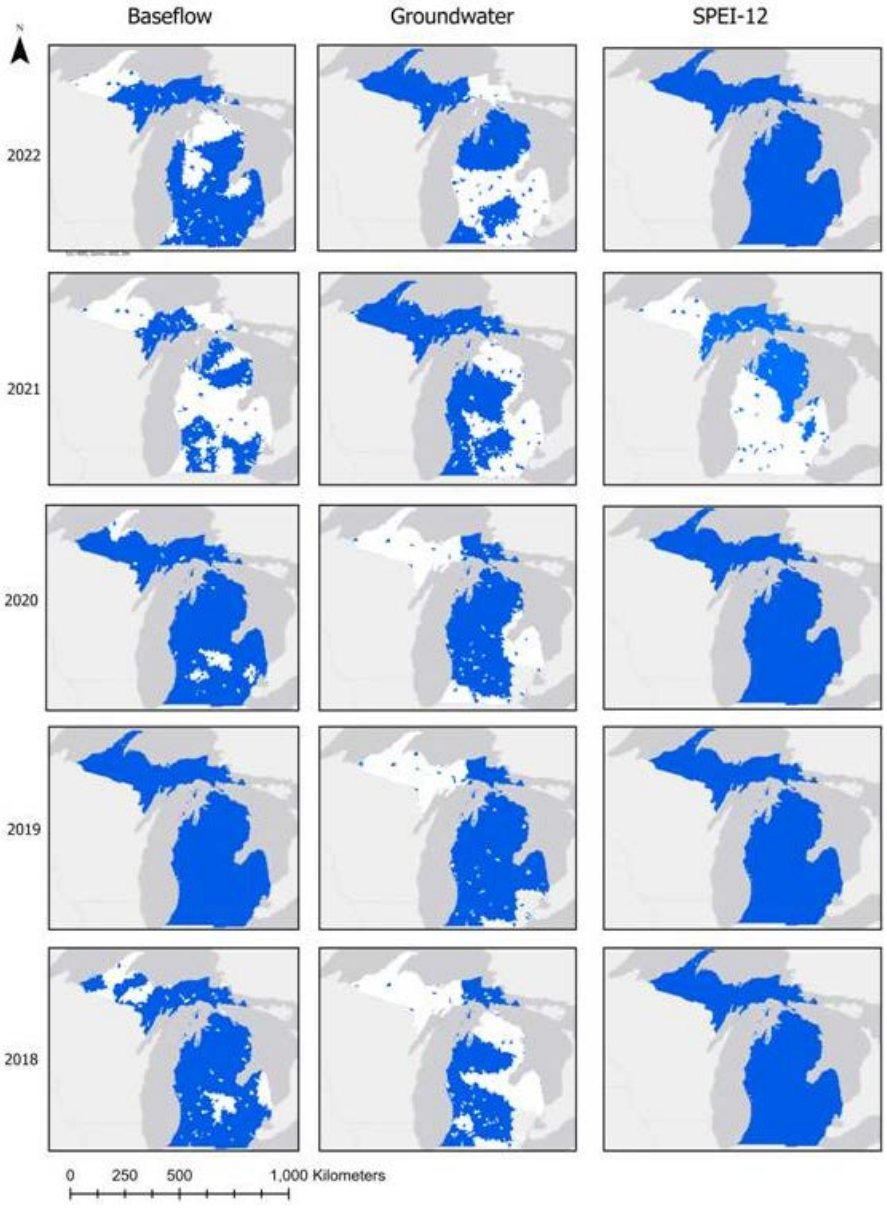

Figure 7. Spatial timeline of maps for 10 years.

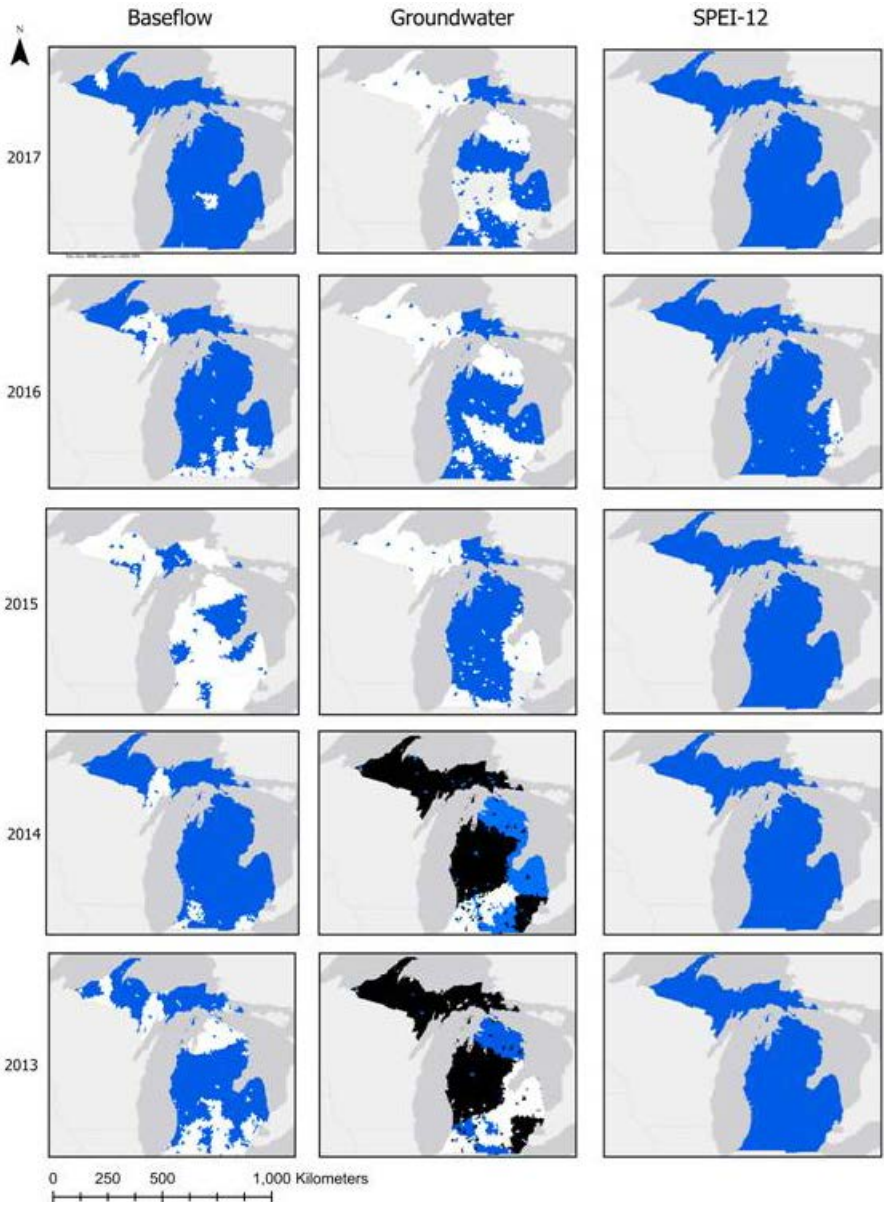

Figure 8. Spatial timeline of maps for 10 years.

5. Discussion

5.1. Isolate Sign Change

In examining the variability in isolated sign changes among standardized baseflow (SDBF), standardized precipitation-evapotranspiration index (SPEI), and standardized groundwater (SDGW) across different time periods, it is evident that baseflow exhibits notably higher variability compared to SPEI and SDGW. This increased variability in SDBF can be attributed to several key factors inherent to baseflow dynamics. Baseflow is directly influenced by groundwater contributions, which are affected by a range of localized hydrological factors such as changes in groundwater recharge rates, aquifer characteristics, and land use impacts [35]. For

instance, research has shown that baseflow can be highly responsive to changes in land use and land cover, with urbanization and agricultural practices significantly altering recharge rates and runoff patterns [35]. Unlike SPEI, which is an integrated index reflecting combined effects of precipitation and potential evapotranspiration, baseflow exhibits greater fluctuations due to its sensitivity to these localized hydrological changes [36].

Moreover, the longer historical period of record for SDBF (1960 - 2022) compared to the more recent 2013 - 2022 period for SDGW may also contribute to the observed variability (**Figures 4-6**). Research by Welsh *et al.*, 2020 [37] highlights that long-term baseflow records capture a broader range of hydrological conditions and anthropogenic influences, adding to its variability. In contrast, the more stable nature of SDGW and SPEI over their respective periods suggests that their variability is less influenced by localized factors and more reflective of broader-scale climatic trends [10]. Consequently, the greater variability in baseflow underscores its sensitivity to diverse hydrological and environmental changes, highlighting the importance of considering these dynamics when analyzing long-term water resource data.

5.2. Mann Kendall: Baseflow Summary

The Mann-Kendall trend analysis provides insight into these changes over two distinct periods: the long-term period from 1960 to 2022 and a more recent short-term period from 2002 to 2022 (**Figure 3**). The spatial distribution of baseflow trends over the long-term period (1960 to 2022) indicates a predominance of increasing trends in the southern Lower Peninsula, while the Upper Peninsula shows a mix of increasing, no trend, and some decreasing trends. The increasing trends in the southern Lower Peninsula could be attributed to a combination of factors. Firstly, this region has undergone significant agricultural expansion and urbanization, both of which can influence baseflow. Agricultural practices often involve the use of tile drainage systems, which can increase the rate at which water enters streams and rivers, leading to higher baseflow levels over time [37].

Additionally, the southern Lower Peninsula's geology and soil composition may contribute to the observed trends. The region's relatively permeable soils and underlying glacial deposits allow for effective infiltration and recharge of groundwater, which supports sustained baseflow even during dry periods [38]. This contrasts with areas in the Upper Peninsula, where more impermeable bedrock and different land-use patterns may contribute to the observed variability in baseflow trends.

The groundwater trend analysis for the period 2002 to 2022 reveals limited increasing trends, with a notable presence of sites showing no trend and a few with decreasing trends. This could suggest that groundwater levels have generally stabilized or are slightly declining in some regions. The lack of significant increasing trends may reflect the balance between groundwater extraction and recharge, particularly in regions where water use for irrigation and other purposes is high [18]

The decreasing trends observed at certain sites, particularly in the Upper Peninsula, may be indicative of over-extraction or reduced recharge rates. This region, characterized by less intense agricultural activity but with a significant reliance on groundwater for local use, may be experiencing the effects of long-term groundwater depletion [38]. The potential influence of climate change, leading to altered precipitation patterns and reduced snowpack, could also be contributing to these trends by affecting the timing and quantity of groundwater recharge [16] [18] [37].

5.3. Correlation

While we were a little surprised to find that our examination of watershed landcover, including wetlands, forests, urban areas, and agricultural use, as well as watershed location and size, reveals no significant correlations with isolated sign changes. Urbanization and agricultural practices have been shown to alter baseflow patterns through modifications in recharge and runoff processes, yet the impact can vary significantly depending on local hydrogeological conditions [37] [39]. Similarly, our analysis of watershed location and size also yielded insignificant results, which is consistent with findings from Clancy, 2023 [17] who observed that watershed size and geographic location alone do not consistently predict baseflow variability. These results suggest that other factors, possibly including soil characteristics, groundwater dynamics, or historical land use changes, may play a more critical role in influencing baseflow variability. Further research should consider these additional variables to provide a more comprehensive understanding of the factors affecting baseflow in different contexts.

5.4. Baseflow Runs

In the Northern region, the observed positive runs ranging from 5 to 21 years, with notable periods starting in the 1960s and early 2000s, reflect the influence of large-scale climate variability (**Figure 3**). The extended positive runs, such as the 21-year period starting in 2002, correspond with significant precipitation events and changes in snowpack, which are influenced by the region's sensitivity to climatic oscillations like the Pacific Decadal Oscillation and North Atlantic Oscillation [40]-[42]). Conversely, the negative runs beginning in the early 2000s highlight periods of reduced precipitation and potentially higher evaporation rates, which can be influenced by regional climatic shifts and lake-effect processes [18]. These are highlighted in **Figures 4-6** and **Table 3**.

In the Southern region, the baseflow data exhibit longer positive runs from the late 1980s to early 2010s and extended negative runs starting in the 1960s and 1990s (**Figure 5**). These patterns reflect the impacts of significant urban development and increased precipitation during the positive runs, which are consistent with enhanced groundwater recharge due to urbanization and regional precipitation increases [43]. The negative runs, on the other hand, correlate with periods of drought or reduced precipitation, which are documented in historical drought records and reflect broader climate variability [44] [45]. The Southern region's

prolonged periods of both positive and negative baseflow trends underscore the influence of anthropogenic factors and extended climatic conditions.

In the Central region, the variability in baseflow run lengths, including positive runs from 5 to 8 years and negative runs from 6 to 13 years, highlights the transitional hydrological response between the more urbanized Southern region and the natural Northern region (**Figure 6**). The mixed patterns in the Central region may result from a combination of regional climatic influences and localized land use changes [37]. The variability in baseflow trends in this region reflects its position as a zone of interaction between different climatic and hydrological factors, leading to a diverse range of hydrological responses.

Overall, the spatial patterns in baseflow runs across Michigan are influenced by a complex interplay of regional climate variability, urban development, and local hydrological conditions. The distinct regional patterns observed highlight the need to consider both climatic and anthropogenic factors when analyzing baseflow trends.

5.5. Groundwater Runs

The observed patterns in groundwater run lengths across Michigan reveal significant regional variations that can be attributed to differences in climate, hydrology, and land use practices. The consistent start dates for both negative and positive runs around the late 1970s to early 1980s across all regions likely reflect a response to broad climatic shifts during this period, including changes in precipitation patterns and temperature [33] [46]. This period marked the transition from cooler and wetter conditions of the early 20th century to a more variable climate regime, influencing groundwater trends across different regions.

In the Southern region, the longest average lengths of both negative and positive runs suggest a more pronounced response to climatic and anthropogenic influences (**Figure 5**). The extended negative runs in the South, averaging 6 to 7 years, may be linked to significant drought periods and increased groundwater extraction associated with urbanization and population growth [43]. The Southern region's longer positive runs, averaging 7 to 8 years, could be attributed to increased precipitation and improved groundwater recharge due to enhanced stormwater management practices and urban infrastructure development [47].

In contrast, the Central and Northern regions exhibit shorter average lengths for both positive and negative runs (**Figure 4** and **Figure 5**). The Central region's shorter positive runs, averaging 5 to 6 years, and negative runs, averaging about 4 years, may reflect its transitional nature between the more urbanized South and the natural Northern regions. This variability is influenced by a mix of urban and rural land use, affecting groundwater dynamics in a less consistent manner [37]. The Northern region's shorter average run lengths, around 4 to 5 years for positive runs and 5 to 6 years for negative runs, likely result from the region's lower population density and limited anthropogenic impacts, as well as its reliance on snowmelt and lake-effect precipitation which can cause more variable groundwater

responses [18].

Overall, these regional differences in groundwater run lengths highlight the complex interplay between climatic conditions, land use practices, and regional hydrology. The Southern region's longer periods of both positive and negative trends underscore the influence of significant anthropogenic and climatic changes, while the shorter and more variable runs in the Central and Northern regions reflect their diverse environmental and land use contexts.

5.6. SPEI

The regional variations in Standardized Precipitation-Evapotranspiration Index (SPEI) run lengths across Michigan reflect the diverse climatic and hydrological influences at play.

In the Northern region, the diverse range of both positive and negative SPEI run lengths, with average maximum negative runs of approximately 6.2 years and positive runs of about 6.7 years, can be attributed to the region's sensitivity to large-scale climatic variability (**Figure 4**). The Northern region, characterized by its reliance on snowpack and lake-effect precipitation, experiences notable fluctuations in both drought and wet conditions. The extended negative runs starting around 2003 and positive runs beginning in 2013 highlight the impact of recent climatic oscillations such as the Pacific Decadal Oscillation and fluctuations in the North Atlantic Oscillation, which drive significant interannual and interdecadal variability in precipitation and evaporation [18] [40].

In the Central region, the shorter average maximum negative runs of about 3.8 years and the more variable positive runs averaging 5.5 years suggest a climate that is less extreme compared to the Northern and Southern regions (**Figures 4-6**). The Central region's more stable yet variable climate can be attributed to its transitional position between the more extreme climates of the North and South. The relatively shorter negative runs, generally starting between 1961 and 1980, may reflect a period of increased precipitation and groundwater recharge, while the variable positive runs, extending to 2013, indicate periods of both wet and dry conditions influenced by regional climatic patterns and localized land use changes [37].

In contrast, the Southern region's longer periods of both negative (average maximum of 6.2 years) and positive runs (average maximum of 8.0 years) are indicative of significant variability in hydrological conditions (**Figure 5**). The extended runs, with notable starts in the 1960s and extending into the 2000s, reflect the region's susceptibility to long-term climatic shifts and anthropogenic impacts. The Southern region has experienced pronounced droughts and wet periods, influenced by both historical land use changes and shifts in precipitation patterns driven by climate change and urbanization [43]-[45]. The Southern region's longer runs underscore its vulnerability to extended climatic extremes and its complex interactions between local and regional climate factors.

Overall, the observed patterns in SPEI runs across Michigan illustrate how regional climatic conditions, such as reliance on snowpack in the North, transitional

climate in the Central region, and long-term variability in the South, drive differences in hydrological responses. These variations emphasize the importance of considering both climatic influences and regional factors when interpreting hydrological trends.

5.7. Spatial Analysis of SDBF, SDGW, and SPEI

As shown in **Figure 7** and **Figure 8**, the analysis of Standardized Baseflow (SDBF) and Standardized Groundwater (SDGW) in comparison to Standardized Precipitation-Evapotranspiration Index (SPEI) reveals distinct regional patterns in Michigan that highlight the nuanced responses of groundwater and baseflow to climatic variability.

In the Northern region, the discrepancy between SDGW and SDBF is particularly notable. While annual SPEI values generally remain positive, with only isolated drier years in 2016 and 2021, SDGW reveals more pronounced regional dryness, especially in 2016, 2017, 2018, and 2021 [48]. This suggests that SDGW, which reflects groundwater conditions, exhibits delayed responses to short-term climatic variations compared to the more immediate responses of SDBF. This lag in SDGW could be due to the inherent inertia of groundwater systems, which often take longer to reflect changes in precipitation and evapotranspiration due to their subsurface storage and slow recharge rates [49] [50]. The persistence of dryness in the Northern part of the state, even when SDBF and SPEI indicate wetter conditions in 2019 and 2020, underscores the slower adjustment of groundwater levels compared to surface flow.

In contrast, the Southern region demonstrates a closer alignment between SDBF and SDGW, with both metrics reflecting the broader trends observed in SPEI. The Southern region's extended periods of both positive and negative runs, coupled with generally longer durations of positive trends, align with historical observations of increased variability in this region [49] [50]. The extended positive and negative periods in the South likely reflect more significant climatic extremes and anthropogenic influences, such as land use changes, which affect both groundwater recharge and baseflow more directly than in the Northern regions [49]-[52].

The Mann-Kendall trend analysis further highlights these spatial differences. Over the long term (1960 to 2022), increasing trends in baseflow are observed predominantly in the Central and Southern regions, while the Northern region shows no significant trends, consistent with the observed patterns of SDGW [51]. The more pronounced recent trends (2002 to 2022) in the Northern region for SDBF, compared to the long-term stability of SDGW, suggest a shift in hydrological dynamics, possibly driven by recent climatic changes or variations in land use and management practices [38] [51].

6. Conclusions

The analysis of groundwater and baseflow data across Michigan reveals significant

regional variations driven by climatic, geographical, and anthropogenic factors. In the southern region, the strong alignment between increasing trends in groundwater and baseflow is consistent with the impacts of increased precipitation and urbanization. These findings underscore the role of urban development in shaping hydrological responses, particularly in areas experiencing rapid urbanization.

In contrast, the northern region presents a more complex hydrological picture, with notable discrepancies between groundwater and baseflow trends. The divergence observed, where groundwater trends decrease while baseflow remains stable, highlights the influence of the region's unique climatic conditions, including lake-effect processes and variable precipitation patterns.

The central region exhibits mixed hydrological trends, reflecting its transitional nature between the more urbanized south and the natural northern areas. The variability in trends observed here suggests that this region is influenced by a combination of urban and natural factors, making it a zone of interaction where both human activities and natural processes drive hydrological changes.

Due to the limitations arising from inconsistent groundwater data, using groundwater in drought models near the Great Lakes in Michigan is not recommended. The high baseflow contributions from streams allow baseflow data to serve as a proxy for groundwater. Overall, baseflow reflects a mixed response to increased precipitation, indicating instability in water resources and suggesting that conservative measures should be considered. Although we deliberately did not examine seasonal data, excluding groundwater from the dataset would make it more feasible to analyze seasonal trends. This may reveal a clearer relationship between baseflow and precipitation.

Conflicts of Interest

The authors declare no conflicts of interest regarding the publication of this paper.

References

[1] Channell, K., DelPizzo, J., Briley, L., Rood, R., Jorns, J. and Hutchens, K. (2022) Lake Michigan: A Summary of Anticipated Future Climate Conditions. Great Lakes Integrated Sciences and Assessments. https://glisa.umich.edu/wp-content/uploads/2022/09/Michigan_Prospective_Report_2022.pdf

[2] Channell, K., DelPizzo, J., Briley, L., Rood, R., Jorns, J. and Hutchens, K. (2022) Lake Superior: A Summary of Anticipated Future Climate Conditions. Great Lakes Integrated Sciences and Assessments. https://glisa.umich.edu/wp-content/uploads/2022/09/Superior_Prospective_Report_2022.pdf

[3] Byun, K., Chiu, C. and Hamlet, A.F. (2019) Effects of 21st Century Climate Change on Seasonal Flow Regimes and Hydrologic Extremes over the Midwest and Great Lakes Region of the US. *Science of the Total Environment*, **650**, 1261-1277. https://doi.org/10.1016/j.scitotenv.2018.09.063

[4] Steinman, A.D., Uzarski, D.G., Lusch, D.P., Miller, C., Doran, P., Zimnicki, T., *et al.* (2022) Groundwater in Crisis? Addressing Groundwater Challenges in Michigan

(USA) as a Template for the Great Lakes. *Sustainability*, **14**, Article 3008. https://doi.org/10.3390/su14053008

[5] Gronewold, A.D., Fortin, V., Lofgren, B., Clites, A., Stow, C.A. and Quinn, F. (2013) Coasts, Water Levels, and Climate Change: A Great Lakes Perspective. *Climatic Change*, **120**, 697-711. https://doi.org/10.1007/s10584-013-0840-2

[6] Gronewold, A.D. and Stow, C.A. (2014) Unprecedented Seasonal Water Level Dynamics on One of the Earth's Largest Lakes. *Bulletin of the American Meteorological Society*, **95**, 15-17. https://doi.org/10.1175/bams-d-12-00194.1

[7] Bellprat, O., Guemas, V., Doblas-Reyes, F. and Donat, M.G. (2019) Towards Reliable Extreme Weather and Climate Event Attribution. *Nature Communications*, **10**, Article No. 1732. https://doi.org/10.1038/s41467-019-09729-2

[8] Aboelnour, M., Gitau, M.W. and Engel, B.A. (2019) Hydrologic Response in an Urban Watershed as Affected by Climate and Land-Use Change. *Water*, **11**, Article 1603. https://doi.org/10.3390/w11081603

[9] Pielke, R.A., Marland, G., Betts, R.A., Chase, T.N., Eastman, J.L., Niles, J.O., *et al.* (2002) The Influence of Land-Use Change and Landscape Dynamics on the Climate System: Relevance to Climate-Change Policy Beyond the Radiative Effect of Greenhouse Gases. *Philosophical Transactions of the Royal Society of London. Series A: Mathematical, Physical and Engineering Sciences*, **360**, 1705-1719. https://doi.org/10.1098/rsta.2002.1027

[10] Vicente-Serrano, S.M., Beguería, S. and López-Moreno, J.I. (2010) A Multiscalar Drought Index Sensitive to Global Warming: The Standardized Precipitation Evapotranspiration Index. *Journal of Climate*, **23**, 1696-1718. https://doi.org/10.1175/2009jcli2909.1

[11] World Meteorological Organization (2023) SPEI Dataset: Climatic Data and Modeling Tools. http://spei.csic.es/

[12] Bhatt, G., Linker, L., Shenk, G., Bertani, I., Tian, R., Rigelman, J., *et al.* (2023) Water Quality Impacts of Climate Change, Land Use, and Population Growth in the Chesapeake Bay Watershed. *JAWRA Journal of the American Water Resources Association*, **59**, 1313-1341. https://doi.org/10.1111/1752-1688.13144

[13] Hameed, M.M., Razali, S.F.M., Mohtar, W.H.M.W., Rahman, N.A. and Yaseen, Z.M. (2023) Machine Learning Models Development for Accurate Multi-Months Ahead Drought Forecasting: Case Study of the Great Lakes, North America. *PLOS ONE*, **18**, e0290891. https://doi.org/10.1371/journal.pone.0290891

[14] Barlow, P.M., and Leake, S.A. (2012) Streamflow Depletion by Wells-Understanding and Managing the Effects of Groundwater Pumping on Streamflow: U.S. Geological Survey Circular 1376. https://pubs.usgs.gov/circ/1376/

[15] Korus, J.T. and Burbach, M.E. (2009) Analysis of Aquifer Depletion Criteria with Implications for Groundwater Management. *Great Plains Research*, **19**, 187-200. http://www.jstor.org/stable/23780128

[16] Ayers, J.R., Villarini, G., Schilling, K. and Jones, C. (2021) On the Statistical Attribution of Changes in Monthly Baseflow across the U.S. Midwest. *Journal of Hydrology*, **592**, Article ID: 125551. https://doi.org/10.1016/j.jhydrol.2020.125551

[17] Clancy, K.A. (2023) Standardized Baseflow Drought Index Comparison to SPEI in High Baseflow Streams. *Journal of Water Resource and Protection*, **15**, 557-580. https://doi.org/10.4236/jwarp.2023.1511031

[18] Manzano, J.E. and Barkdoll, B.D. (2022) Precipitation and Streamflow Trends in Michigan, USA. *Sustainable Water Resources Management*, **8**, Article No. 56. https://doi.org/10.1007/s40899-022-00606-3

[19] USGS (US Geological Survey) (2024) Web Interface: U.S. Geological Survey National Water Information System Web Site. http://waterdata.usgs.gov/nwis/

[20] Vicente-Serrano, S.M. and National Center for Atmospheric Research Staff (2022) The Climate Data Guide: Standardized Precipitation Evapotranspiration Index (SPEI). https://climatedataguide.ucar.edu/climate-data/standardized-precipitation-evapotranspiration-index-spei

[21] Sloto, R.A. and Crouse, M.Y. (1996) HYSEP-A Computer Program for Stream-flow Hydrograph Separation and Analysis. U.S. Geological Survey Water-Resources Investigations Report 96-4040. http://pubs.er.usgs.gov/publication/wri964040

[22] Troolin, W.D. and Clancy, K. (2016) Comparison of Three Delineation Methods Using the Curve Number Method to Model Runoff. *Journal of Water Resource and Protection*, **8**, 945-964. https://doi.org/10.4236/jwarp.2016.811077

[23] Jenson, S. (1984) Automated Derivation of Hydrological Basin Characteristics from Digital Elevation Data. US Geological Survey Report 14-08-0001-20129. http://topotools.cr.usgs.gov/pdfs/automated-derivation-of-hydrologic-basin-characteristics-from-digital-elevatioin-model-data.pdf

[24] USGS (US Geological Survey) (2019) NED (National Elevation Data) 2020 Elevation. SDE Raster Digital Data. http://nationalmap.gov/eleva

[25] USGS (US Geological Survey) (2020) NLCD (National Land Cover Database) 2020 Land Cover. SDE Raster Digital Data. https://www.mrlc.gov/

[26] U.S. Geological Survey (2024) Hydrological Unit Codes (HUC). Watershed Boundary Dataset. https://www.usgs.gov/national-hydrography/watershed-boundary-dataset

[27] Vicente-Serrano, S.M., López-Moreno, J.I., Beguería, S., Lorenzo-Lacruz, J., Azorin-Molina, C. and Morán-Tejeda, E. (2012) Accurate Computation of a Streamflow Drought Index. *Journal of Hydrologic Engineering*, **17**, 318-332. https://doi.org/10.1061/(asce)he.1943-5584.0000433

[28] Wang, Y., Kong, Y., Chen, H. and Ding, Y. (2020) Spatial-Temporal Characteristics of Drought Detected from Meteorological Data with High Resolution in Shaanxi Province, China. *Journal of Arid Land*, **12**, 561-579. https://doi.org/10.1007/s40333-020-0066-x

[29] Hayes, M.J., Svoboda, M.D., Wilhite, D.A. and Vanyarkho, O.V. (1999) Monitoring the 1996 Drought Using the Standardized Precipitation Index. *Bulletin of the American Meteorological Society*, **80**, 429-438. https://doi.org/10.1175/1520-0477(1999)080<0429:mtduts>2.0.co;2

[30] McLeod, A.I. (2023). Kendall: Kendall Rank Correlation and Mann-Kendall Trend Test. Version 2.2. https://cran.r-project.org/web/packages/Kendall/index.html

[31] Hirsch, R.M., Slack, J.R. and Smith, R.A. (1982) Techniques of Trend Analysis for Monthly Water Quality Data. *Water Resources Research*, **18**, 107-121. https://doi.org/10.1029/wr018i001p00107

[32] Hamed, K.H. and Ramachandra Rao, A. (1998) A Modified Mann-Kendall Trend Test for Autocorrelated Data. *Journal of Hydrology*, **204**, 182-196. https://doi.org/10.1016/s0022-1694(97)00125-x

[33] Burn, D.H. and Hag Elnur, M.A. (2002) Detection of Hydrologic Trends and Variability. *Journal of Hydrology*, **255**, 107-122. https://doi.org/10.1016/s0022-1694(01)00514-5

[34] Caloiero, T., Caloiero, P. and Frustaci, F. (2018) Long-Term Precipitation Trend Analysis in Europe and in the Mediterranean Basin. *Water and Environment Journal*, **32**, 641.

[35] Bloomfield, J.P., Gong, M., Marchant, B.P., Coxon, G. and Addor, N. (2021) How Is Baseflow Index (BFI) Impacted by Water Resource Management Practices? *Hydrology and Earth System Sciences*, **25**, 5355-5379. https://doi.org/10.5194/hess-25-5355-2021

[36] Gao, Y., Chen, J., Luo, H. and Wang, H. (2020) Prediction of Hydrological Responses to Land Use Change. *Science of the Total Environment*, **708**, Article ID: 134998. https://doi.org/10.1016/j.scitotenv.2019.134998

[37] Welsh, M.K., Vidon, P.G. and McMillan, S.K. (2020) Stream and Floodplain Restoration Impacts Riparian Zone Hydrology of Agricultural Streams. *Environmental Monitoring and Assessment*, **192**, Article No. 85. https://doi.org/10.1007/s10661-019-7795-3

[38] Cherkauer, K.A. and Sinha, T. (2010) Hydrologic Impacts of Projected Future Climate Change in the Lake Michigan Region. *Journal of Great Lakes Research*, **36**, 33-50. https://doi.org/10.1016/j.jglr.2009.11.012

[39] Marx, C., Tetzlaff, D., Hinkelmann, R. and Soulsby, C. (2023) Effects of 66 Years of Water Management and Hydroclimatic Change on the Urban Hydrology and Water Quality of the Panke Catchment, Berlin, Germany. *Science of the Total Environment*, **900**, Article ID: 165764. https://doi.org/10.1016/j.scitotenv.2023.165764

[40] Deser, C. and Phillips, A. (2017) An Overview of Decadal-Scale Sea Surface Temperature Variability in the Observational Record. *Past Global Changes Magazine*, **25**, 2-6.

[41] Grote, T. and Suriano, Z. (2024) Temporal and Spatial Patterns of Hydroclimate Variability Related to the Pacific Decadal Oscillation in Michigan, USA. *Physical Geography*. https://doi.org/10.1080/02723646.2024.2315642

[42] Masuda, S. (2002) Role of the Ocean in the Decadal Climate Change in the North Pacific. *Journal of Geophysical Research*: *Oceans*, **107**, 17-1-17-18. https://doi.org/10.1029/2002jc001420

[43] Jiang, Y., Fu, P. and Weng, Q. (2015) Assessing the Impacts of Urbanization-Associated Land Use/Cover Change on Land Surface Temperature and Surface Moisture: A Case Study in the Midwestern United States. *Remote Sensing*, **7**, 4880-4898. https://doi.org/10.3390/rs70404880

[44] Zhang, Y., Chiew, F.H.S., Li, M. and Post, D. (2018) Predicting Runoff Signatures Using Regression and Hydrological Modeling Approaches. *Water Resources Research*, **54**, 7859-7878. https://doi.org/10.1029/2018wr023325

[45] Cao, Q., Liu, Y., Georgescu, M. and Wu, J. (2020) Impacts of Landscape Changes on Local and Regional Climate: A Systematic Review. *Landscape Ecology*, **35**, 1269-1290. https://doi.org/10.1007/s10980-020-01015-7

[46] Mann, M.E., Bradley, R.S. and Hughes, M.K. (1998) Global-Scale Temperature Patterns and Climate Forcing over the Past Six Centuries. *Nature*, **392**, 779-787. https://doi.org/10.1038/33859

[47] Locke, K.A. (2024) Impacts of Land Use/Land Cover on Water Quality: A Contemporary Review for Researchers and Policymakers. *Water Quality Research Journal*, **59**, 89-106. https://doi.org/10.2166/wqrj.2024.002

[48] Mishra, A.K. and Singh, V.P. (2010) A Review of Drought Concepts. *Journal of Hydrology*, **391**, 202-216. https://doi.org/10.1016/j.jhydrol.2010.07.012

[49] Fienen, M.N., Nolan, B.T., Kauffman, L.J. and Feinstein, D.T. (2018) Metamodeling for Groundwater Age Forecasting in the Lake Michigan Basin. *Water Resources Research*, **54**, 4750-4766. https://doi.org/10.1029/2017wr022387

[50] Anurag, H. and Ng, G.C. (2022) Assessing Future Climate Change Impacts on Groundwater Recharge in Minnesota. *Journal of Hydrology*, **612**, Article ID: 128112. https://doi.org/10.1016/j.jhydrol.2022.128112

[51] Krakauer, N.Y., Lakhankar, T. and Hudson, D. (2019) Trends in Drought over the Northeast United States. *Water*, **11**, Article 1834. https://doi.org/10.3390/w11091834

[52] Sivapalan, M., Savenije, H.H.G. and Blöschl, G. (2012) Socio-Hydrology: A New Science of People and Water. *Hydrological Processes*, **26**, 1270-1276. https://doi.org/10.1002/hyp.8426